

NONSYMMETRIC MOVING BREATHER COLLISIONS IN THE PEYRARD-BISHOP DNA MODEL

A. ALVAREZ AND F. ROMERO

Grupo de Física No Lineal. Facultad de Física. Universidad de Sevilla.
Avda. Reina Mercedes, s/n. 41012-Sevilla (Spain)

J.M. ROMERO AND J.F.R. ARCHILLA

Grupo de Física No Lineal. ETSII. Universidad de Sevilla.
Avda. Reina Mercedes, s/n. 41012-Sevilla (Spain)

(Communicated by the associate editor name)

ABSTRACT. We study nonsymmetric collisions of moving breathers (MBs) in the Peyrard-Bishop DNA model. In this paper we have considered the following types of nonsymmetric collisions: head-on collisions of two breathers traveling with different velocities; collisions of moving breathers with a stationary trapped breather; and collisions of moving breathers traveling with the same direction. The various main observed phenomena are: one moving breather gets trapped at the collision region, and the other one is reflected; breather fusion without trapping, with the appearance of a new moving breather; and breather generation without trapping, with the appearance of new moving breathers traveling either with the same or different directions. For comparison we have included some results of a previous paper concerning to symmetric collisions, where two identical moving breathers traveling with opposite velocities collide. For symmetric collisions, the main observed phenomena are: breather generation with trapping, with the appearance of two new moving breathers with opposite velocities and a stationary breather trapped at the collision region; and breather generation without trapping, with the appearance of new moving breathers with opposite velocities. A common feature for all types of collisions is that the collision outcome depends on the internal structure of the moving breathers and the exact number of pair-bases that initially separates the stationary breathers when they are perturbed. As some nonsymmetric collisions result in the generation of a new stationary trapped breather of larger energy, the trapping phenomenon could play an important part of the complex mechanisms involved in the initiation of the DNA transcription processes.

1. Introduction. The DNA molecule is a discrete system consisting of many atoms having a quasi-one-dimensional structure. It can be considered as a complex dynamical system, and, in order to investigate some aspects of the dynamics and the thermodynamics of DNA, several mathematical models have been proposed.

Among them, it is worth remarking the Peyrard–Bishop model [27, 16] introduced for the study of DNA thermal denaturation. In this model the DNA molecule is

2000 *Mathematics Subject Classification.* Primary: 70Kxx, 82C22; Secondary: 92D20.

Key words and phrases. Peyrard-Bishop DNA model, DNA, Klein-Gordon chains, Moving breathers.

All authors are supported by Spanish MICINN grant FIS2008-04848.

considered as a Klein-Gordon chain of oscillators, and have been used extensively for the study of the dynamical properties.

The study of discrete breathers (DBs), in chains of oscillators, is an active research field in nonlinear physics [3, 2, 1, 19]. These vibrational entities are rather generic in models of Klein-Gordon and FPU lattices [23, 7, 30, 28].

Under certain conditions, DBs can be set in motion if they experience appropriate perturbations [10, 8], and they are called *moving breathers* (MBs). There are no exact solutions for MBs, but they can be obtained by means of numerical calculations. The conditions for the existence of MBs in Klein-Gordon chains depend on the exact details of both the on-site and the inter-site potentials. One of the most thoroughly studied Klein-Gordon models where MBs appear is the Hamiltonian Klein-Gordon chain with Morse on-site potential and harmonic coupling potential [11, 13, 14].

In the Peyrard-Bishop model, the existence of DBs has been demonstrated [16], and DBs are thought to be the precursors of the bubbles that appear prior to the transcription processes in which large fluctuations of energy have been experimentally observed. Some studies about the existence and properties of MBs in the Peyrard-Bishop model including dipole-dipole dispersive interaction are carried out in [11] [4].

In a DNA molecule, MBs should appear at arbitrary positions, then, it is natural to be interested in their collisions. The study of collisions of MBs in FPU chains was initiated in [18]. However, in Klein-Gordon chains, the studies were initially limited to the interaction of moving low-amplitude breathers with stationary high-amplitude ones [15, 21, 20], or to the interaction between quasi-periodic moving breathers in dissipative lattices [25]. More recently, some results have been obtained considering symmetric head-on collisions in a Klein-Gordon chain with the Morse potential and harmonic coupling potential [5, 6]. These results can be interpreted in the context of DNA because the on-site potential of the Peyrad Bishop model is a Morse potential.

The aim of this paper is to get some insight into the detailed mechanisms and possible outcomes of nonsymmetric collisions in the Peyrard-Bishop model.

This article is organized as follows. Sec. 2 presents the Peyrard-Bishop model, describes the technics for generating MBs and the different types of collisions. Sec. 3 presents the results corresponding to nonsymmetric collisions in the Peyrard-Bishop model. Sec. 4 presents for comparison the results obtained for symmetric collisions as applied to the Peyrard-Bishop model. Finally, the conclusions are presented in Sec. 5.

2. Moving breathers in the Peyrad-Bishop model. The Peyrard-Bishop DNA model corresponds to the Hamiltonian:

$$H = \sum_{n=1}^N \left[\frac{1}{2} m \dot{u}_n^2 + D(e^{-bu_n} - 1)^2 + \frac{1}{2} \varepsilon_0 (u_{n+1} - u_n)^2 \right], \quad (1)$$

the term $\frac{1}{2} m \dot{u}_n^2$ represents the kinetic energy of the nucleotide of mass m at the n^{th} site of the chain, and u_n is the variable representing the transverse stretching of the hydrogen bond connecting the base at the n^{th} site. The Morse potential, i.e., $D(e^{-bu_n} - 1)^2$, represents the interaction energy due to the hydrogen bonds within the base pairs, D being the well depth, which corresponds to the dissociation energy of a base pair, and b^{-1} is related to the width of the well. The stacking energy is $\frac{1}{2} \varepsilon_0 (u_{n+1} - u_n)^2$, where ε_0 is the stacking coupling constant.

In scaled variables this Hamiltonian can be written as:

$$H = \sum_n \left[\frac{1}{2} \dot{u}_n^2 + V(u_n) + \frac{1}{2} \varepsilon (u_n - u_{n+1})^2 \right], \quad (2)$$

where u_n represents the displacement of the n^{th} pair-base from the equilibrium position, ε is the coupling parameter and $V(u_n)$ is:

$$V(u_n) = \frac{1}{2} (\exp(-u_n) - 1)^2. \quad (3)$$

Time-reversible, stationary breathers can be obtained using methods based on the anti-continuous limit [24]. Initially, $\dot{u}_n = 0, \forall n$, and the displacements of a stationary breather centered at n_0 are denoted by $\{u_{SB,n}\}$. A moving breather $\{u_{MB,n}\}$ can be obtained with an appropriate perturbation of the stationary breather. One possibility consists in modifying its initial conditions as follows:

$$\begin{aligned} u_{MB,n}^0 &= u_{SB,n} \cos(\alpha(n - n_0)) \\ \dot{u}_{MB,n}^0 &= \pm u_{SB,n} \sin(\alpha(n - n_0)). \end{aligned} \quad (4)$$

The plus-sign gives rise to breathers traveling towards the positive direction, and the minus-sign towards the opposite one. This procedure, taken from the DNLS context [26, 12], works as well as the marginal-mode method [10, 8] and gives good mobility for a large range of ε values. We take Eqs. (4) as the initial conditions for integrating the dynamical equations using a symplectic algorithm [29], and take periodic boundary conditions.

The characteristics and internal structure of a MB depend on the potentials $V(u_n)$, also on the specific form of the perturbation given to the stationary breather. In our case, the parameter α is involved in this perturbation, it represents the difference of phase between two neighboring oscillators (pair-bases) and we will refer to it as the *wave number*. We have shown that the translational velocity and the translational kinetic energy of the MB increase with α .

Moving breathers are not so well characterized as solitons, as they are obtained numerically by a perturbation and slowly decay and change in time. However, we still speak loosely of the internal structure of moving breathers to indicate that they have been obtained with different parameters ω_b and α . Also this internal structure changes with time which leads to different outcomes of the collisions by simply changing the distance or time traveled until a collision. This lack of characterization will make difficult to understand the mechanisms for the different collisions.

We call N_c the number of pair-bases separating initially the centers of the two DBs, and we distinguish two types of collisions: a) on-site collisions (OS), if N_c is an odd number, that is, the middle of the initial separation coincides with a pair-base; and b) inter-site collisions (IS), if N_c is even.

3. Nonsymmetric collision simulations. The study begins generating two stationary breathers, with the same frequency, separated by a given number of pair-bases between their centers. To obtain MBs, each breather should be perturbed using the initial conditions given by Eqs. (4). To obtain nonsymmetric collisions each perturbation must be different. Hereafter, the MBs are called MB₁ and MB₂, and they are perturbed with the α values denoted by α_1 and α_2 , respectively. In this section we consider three different types of nonsymmetric collisions: a) collisions of

two moving breathers traveling with different velocities and different directions: α_1 and α_2 have different modulus but the sign applied to the perturbation is different; b) collisions of moving breathers with a stationary breather: $\alpha_1 \neq 0$ and $\alpha_2 = 0$; and c) collisions of moving breathers traveling with different velocities and the same direction: α_1 and α_2 have different modulus and the sign of the perturbation is the same. The calculations have been tested using different system sizes, to make sure that the results are not modified by boundary effects (most of the simulations have been done with $N > 400$). In this paper we have taken $N_c = 50$, but we have observed that the outcomes have a great sensitivity with respect to this number.

The breather frequency ω_b is below the phonon band because the Morse on-site potential is soft.

The lowest frequency of the phonon band corresponds to the phonon where all the oscillators vibrate in phase with small amplitude. Its frequency is equal to the linear frequency of an isolated oscillator given by $\omega_0 = V''(0)^{1/2}$.

For breathers with small amplitude the system is close to the linear limit, and their frequency is close to ω_0 . Therefore, $|\omega_0 - \omega_b|$ is a measure of how far the system is from the linear regime. In this paper we consider the frequency $\omega_b = 0.8$ which represents an intermediate degree of nonlinearity. For the coupling constant ε we have taken a range of values consistent with real DNA [11].

3.1. Head-on collisions of moving breathers with different velocities. For these collisions MB_1 and MB_2 travel with opposite directions. We have observed three main scenarios that correspond two different perturbations.

1. *Breather fusion with the generation of a new moving breather:*

Fig. 1 shows an example of this type of head-on collisions, corresponding to $\alpha_1 = 0.048$ and $\alpha_2 = 0.046$.

2. *Generation of two new breathers traveling in the same direction:*

An example, corresponding to $\alpha_1 = 0.042$ and $\alpha_2 = 0.061$, is shown in Fig. 2.

3. *One breather gets trapped and the other one is reflected:*

Fig. 3 shows an example corresponding to $\alpha_1 = 0.042$ and $\alpha_2 = 0.131$.

We have observed a great sensitivity with respect to the α_1 and α_2 values, that is, the outcome can be different with these values varying by a small amount.

Note that the fusion of two breathers is only one of the possible outcomes. This is a different from the results obtained in Ref. [15], where fusion is the generic outcome. The differences may be due to a different on-site potential and to the fact that they always collide small amplitude breathers, close to the linear regime, while ours at $\omega_b = 0.8$ are quite far from it.

3.2. Collisions of a moving breather with a static stationary breather. In this case one of the stationary breathers is not perturbed and there is only a MB that collides with the static one. We have observed three basic scenarios:

1. *One breather gets trapped and the other one is reflected:*

Fig. 4(a) shows an example of these type of collisions with $\alpha = 0.078$, $\omega_b = 0.8$ and $\varepsilon = 0.25$.

2. *Generation of two new breathers traveling with different directions:*

The collision produces two new emerging MBs traveling in opposite directions. Fig. 4(b) corresponds to $\alpha = 0.084$, $\omega_b = 0.8$ and $\varepsilon = 0.25$.

3. *Generation of two new breathers traveling with the same direction:*

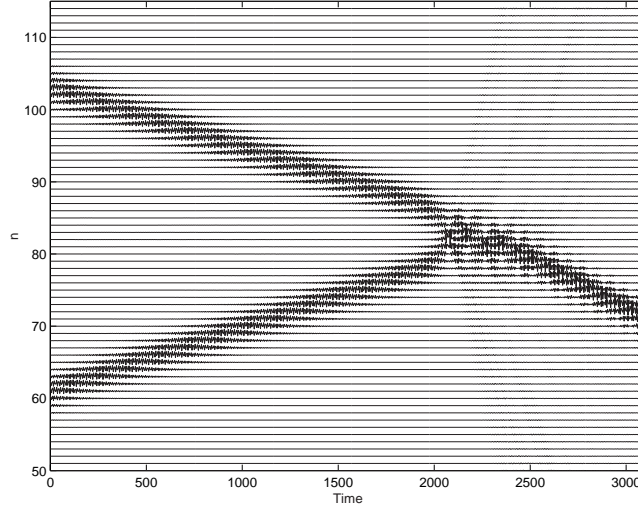


FIGURE 1. An example of a head-on collision with $\varepsilon = 0.14$ and $\omega_b = 0.8$. Displacement from the n -th equilibrium position versus time corresponding to $\alpha_1 = 0.048$ and $\alpha_2 = 0.046$.

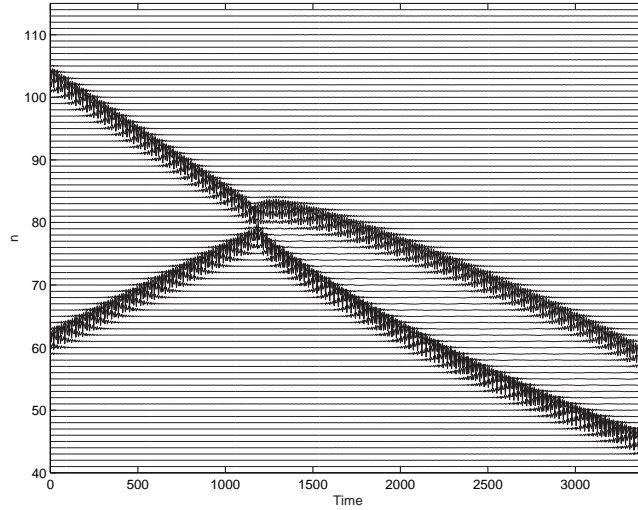


FIGURE 2. An example of a head-on collision with $\varepsilon = 0.15$ and $\omega_b = 0.8$. Displacement from the n -th equilibrium position versus time corresponding to $\alpha_1 = 0.042$ and $\alpha_2 = 0.061$.

An example of this collision with $\alpha = 0.174$, $\omega_b = 0.8$ and $\varepsilon = 0.25$ is shown in Fig. 4(c).

For a given value of ε , the outcome changes among the three above mentioned structures as the parameter α takes different values within the interval $[0.03, 0.2]$. If the coupling constant ε is changed, for example $\varepsilon = 0.13$ the scenario (2) is obtained for $\alpha = 0.06$ and the scenario (3) for both $\alpha = 0.084$ and $\alpha = 0.174$.

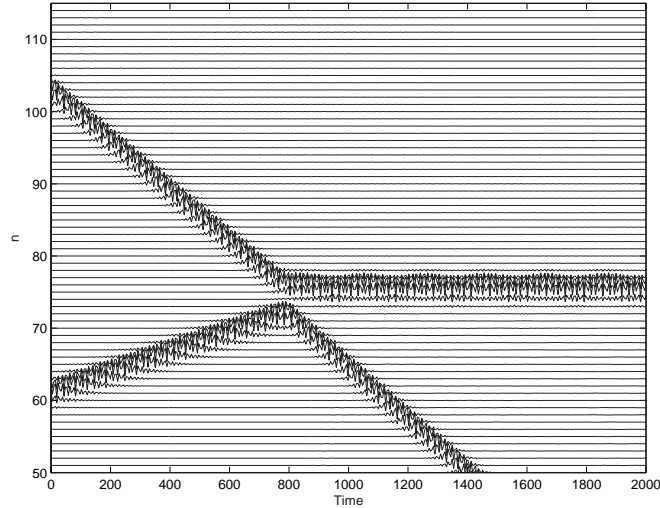


FIGURE 3. An example of a head-on collision with $\varepsilon = 0.15$ and $\omega_b = 0.8$. Displacement from the n -th equilibrium position versus time corresponding to $\alpha_1 = 0.042$ and $\alpha_2 = 0.131$.

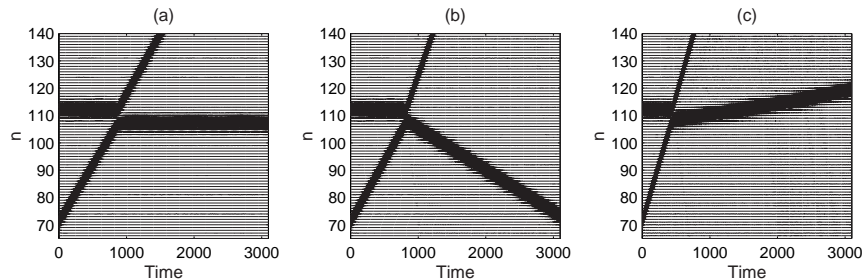


FIGURE 4. An example of the three basic scenarios with $\omega_b = 0.8$ and $\varepsilon = 0.25$. Displacement from the n -th equilibrium position versus time for three different values of the translational kinetic energy, corresponding to: (a) $\alpha = 0.078$; (b) $\alpha = 0.084$; (c) $\alpha = 0.174$.

3.3. Collision between two moving breathers traveling with the same direction. These type of collisions appear when two MBs are launched with the same direction and different velocities. We have observed also three different basic scenarios, they are similar to those shown in Fig. 4. The simulations have been done with $\alpha_1 = 0.2$ and $\alpha_2 \in [0.03, 0.15]$. The system changes among them as the parameter α_2 takes different values. An example of this type of collision is shown in Fig. 5 with $\varepsilon = 0.18$, $\omega_b = 0.8$, $\alpha_1 = 0.2$ and three values of α_2 . Fig. 5(a) with $\alpha_2 = 0.032$; Fig. 5(b) with $\alpha_2 = 0.034$ and Fig. 5(c) with $\alpha_2 = 0.042$. The outcome corresponding to the generation of a stationary trapped breather disappears for high enough values of ε . As in the other types of collisions, the system is quite sensitive to the α values and to N_c .

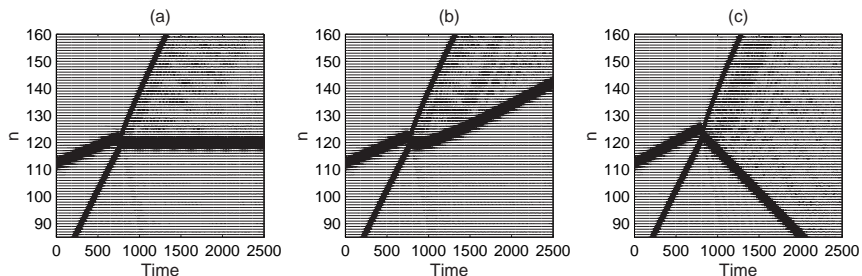


FIGURE 5. An example of the three basic scenarios with $\omega_b = 0.8$, $\varepsilon = 0.18$ and $\alpha_1 = 0.2$. Displacement from the n -th equilibrium position versus time for three different values of the translational kinetic energy of the MB_2 corresponding to: (a) $\alpha_2 = 0.032$; (b) $\alpha_2 = 0.034$; (c) $\alpha_2 = 0.042$.

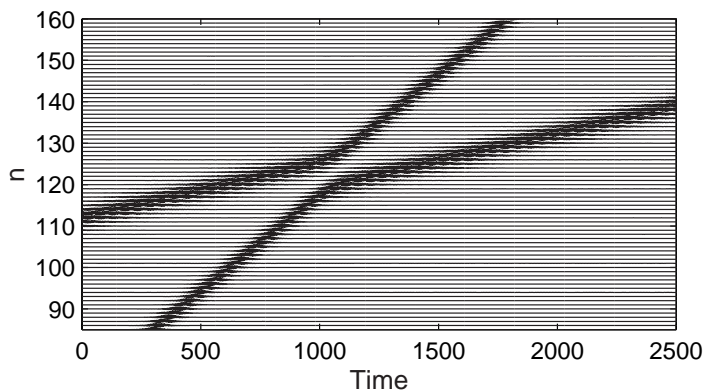


FIGURE 6. Displacement from the n -th equilibrium position versus time for $\omega_b = 0.95$, $\varepsilon = 0.18$, $\alpha_1 = 0.2$ and $\alpha_2 = 0.054$.

For breather frequencies around the value $\omega_b = 0.95$, which is close to the frequency of an isolated oscillator in the linear regime, we find only a single outcome for each value of ε , varying α_2 : the collision produces two breathers moving in the same direction and with almost the same velocities of the incident breathers. An example is shown in Fig. 6 for $\varepsilon = 0.18$, $\alpha_1 = 0.2$ and $\alpha_2 = 0.054$.

4. A comparison with the results for symmetric collisions. In a recent paper [6] we presented an extensive study of symmetric collisions in Klein-Gordon chains. In this section we present a summary of those results in order to establish a comparison with the results for nonsymmetric collisions.

For obtaining symmetric collisions it is necessary to generate two stationary breathers, with the same frequency, separated by a given number of pair-bases between their centers. Both breathers are in phase, that is, before the perturbation each breather is always like the mirror image of the other one. The perturbation should be given simultaneously to both breathers using the initial conditions given by Eqs. (4), with the plus sign for one breather and the minus sign for the other

one. In this way the MBs travel with the same modulus of velocity, but opposite directions, and they are in phase.

We can consider different symmetric collisions varying the parameter α and maintaining fixed the number N_c , in this way we can find the possible outcomes and test the sensitivity with respect to α . Also, we can analyze different symmetric collisions with a fixed value of α and different values of N_c , in this way we can test the sensitivity with respect to N_c as the colliding MBs are always identical. When N_c changes, the dynamical states of the MBs change when the collision begins. Thus, this approach is complementary to the previous one.

We write

$$N_c = N_o + jj, \quad (5)$$

where N_o is a fixed number to guarantee that the breathers are initially far apart, and jj is a positive even number. Thus, for OS collisions N_o is odd, and for IS collisions N_o is even.

Although the MBs are identical when jj varies, the time passed between the initial perturbation and the initiation of the collision increases with jj . The possible different outcomes should be due to the different internal states of motion of the MBs when they collide.

Our results relative to OS symmetric collisions can be summarized as follow:

1. *MB generation without trapping:*

The collision produces only two new symmetric MBs, with almost the same velocity as that of the colliding breathers. This is shown in Fig. 7(a) for $\alpha = 0.32$ and $N_c = 41$.

2. *MB generation with trapping:*

The collision produces new breathers, a trapped one located at the collision region, and two new symmetric MBs, as Fig. 7(b) shows for $\alpha = 0.32$ and $N_c = 43$. The trapped breather contains most of the initial energy.

Varying the parameter jj , it is possible to obtain a noticeable attenuation of the amplitude of the trapped breather as it is shown in Fig. 7(c) which corresponds to $N_c = 45$. In this case the emerging MBs contain most of the initial energy.

The total energy transported by the colliding MBs is distributed after the collision: some part corresponds to the energy of the trapped breather, another part to the emerging MBs, and a small fraction of the energy is transferred to the lattice in the form of phonon radiation. In order to illustrate this phenomenon, we have studied the evolution of the “central energy, defined in our study as the energy of eleven particles around the collision region. This number of particles has been selected because it corresponds to the typical size of a discrete breather with the parameters used. Fig. 8 shows the evolution of the central energy for the three cases considered in Fig. 7.

Before the collision the central energy is zero; after the initiation of the collision it increases quickly, up to a value very close to the sum of the incident MB energies; the subsequent decrease of the central energy is caused by the appearance of new emerging MBs (some of them of short life) and by the phonon radiation.

Fig. 8 shows the evolution of the trapped energy corresponding to three collisions of Fig. 7. For the case with $jj = 0$, the trapped energy is close to zero. whereas for the cases with $jj = 2$ and $jj = 4$, most of the energy remains trapped after the collision.

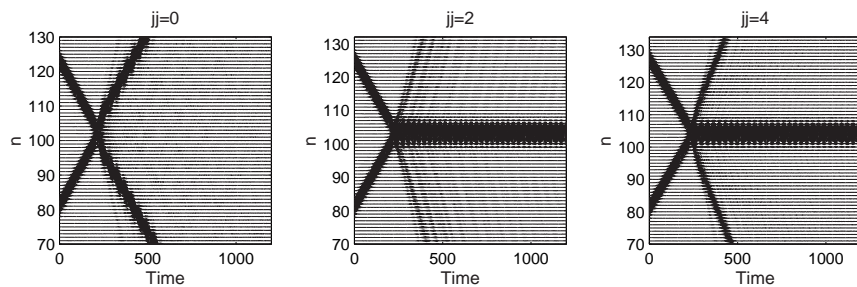


FIGURE 7. Displacements versus time for three OS symmetric collisions corresponding to (a) $jj = 0$; (b) $jj = 2$ and (c) $jj = 4$ with the fixed value $\alpha = 0.138$. Coupling parameter $\varepsilon = 0.32$ and breather frequency $\omega_b = 0.8$.

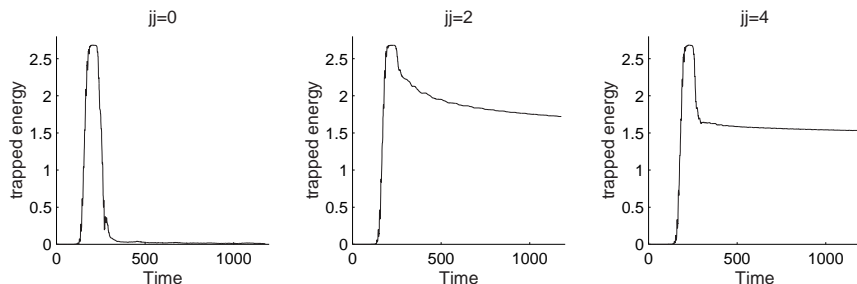


FIGURE 8. Trapped energy versus time corresponding, respectively, to the three collisions of Fig. 7.

The qualitative results are similar for other values of (ε, α) . For a given value of the coupling parameter ε , MB generation without trapping begins to appear for α over a certain value. This value increases when the coupling parameter ε decreases and with a small value of ε , for example with $\varepsilon = 0.15$, there is always trapping with MB generation.

We have observed that there are no significant qualitative differences between the outcomes of OS and IS collisions.

We can see now that the scenarios for symmetric and nonsymmetric collisions are quite different. For symmetric collisions, symmetry is always maintained and a trapped breather can appear or not. For nonsymmetric collisions there are a variety of possible outcomes, some of which are very interesting. It is possible a fusion of two MBs given rise to a new MB as in Fig. 1; two new MBs traveling as a bond state as in Fig. 2; a stationary trapped breather can appears accompanied by a new MB as in Fig. 3 or Fig. 5(a); maintenance of a static breather as in Fig. 4(a); generation of new MBs traveling with the same direction as in Fig. 4(c) or Fig. 5(b).

Generally, the simulations show that the outcome is strongly sensitive to the exact dynamical states of the MBs just before the collision. Fixing the values of the parameters α and varying N_c , the only difference between two collisions is the time passed between the initial perturbation and the initiation of the collision. There exists a great sensitivity with respect to N_c as can be seen, for example, in Fig. 7

for the case of symmetric collisions. This sensitivity exists also for nonsymmetric collisions.

The outcome is strongly sensitive to the internal structure of the MBs, which change as α change. Thus, fixing the value of N_c , the outcome is very sensitive with respect to the α values.

5. Conclusions. In this paper, we have studied, by means of numerical simulations, the nonsymmetric collisions of moving discrete breathers in the the Peyrad-Bishop DNA model. We have taken as varying parameters the stacking coupling constant, the common breather frequency, the velocities of the moving breathers, and the number of pair-bases that initially separates the moving breathers when they are set in motion. For the comparison, we have presented a summary of the results for symmetric collisions which were published in our recent paper [6].

We have considered the following types of nonsymmetric collisions: head-on collisions of two moving breathers traveling with different velocities; collisions of moving breathers with a stationary trapped breather; and collisions of moving breathers traveling with the same direction.

The main observed scenarios for nonsymmetric collisions are: trapping of one of the moving breather at the collision region, and reflection of the other one; breather fusion without trapping, with the appearance of a new moving breather; two new MBs traveling as a bond state; breather generation without trapping, with the appearance of new moving breathers traveling either with the same or different directions.

The main observed scenarios for symmetric collisions are: breather generation with trapping, with the appearance of two new moving breathers with opposite velocities and a stationary breather trapped at the collision region; breather generation without trapping, with the appearance of new moving breathers with opposite velocities. As can be observed the variety of qualitatively different collisions outcomes is wider for nonsymmetric collisions in comparison to symmetric ones.

This could be explained considering that the symmetry of conditions sets a constraint on the energy and momentum exchange between the colliding DBs.

We emphasize an important difference between these two scenarios: breather fusion is impossible for symmetric collisions, whereas for nonsymmetric collisions a new MB can appear with larger energy. This phenomenon could play an important part of the complex mechanisms involved in the initiation of the DNA transcription processes.

An important conclusion is that the types of outcomes depend very sensitively on the initial separation between the breathers, that is, the number of pair-bases that separates the stationary breathers when they are set in motion. Also, with respect to their velocities, which are related to the magnitude of the perturbation given to set them in motion.

The consequence for a physical system is that all the possible outcomes will happen with different probabilities. It makes also difficult to produce a determined outcome for a single event.

The exact mechanisms of energy and momentum exchange between colliding breathers are still unknown, they constitute a challenge for future research. In the study of solitary wave collisions in non-integrable models, at least two generic mechanisms of energy exchange between colliding solitons have been reported. The first one operates through the excitation of the soliton's internal modes, as appears

in the case of kink-antikink interactions in ϕ^4 theory [9]. The second mechanism, recently discovered studying three soliton collisions [17], is the radiationless energy exchange between the colliding solitons in weakly perturbed integrable systems. It takes place in near-separatrix of the multisoliton solutions of the corresponding integrable equations. An advance in the understanding of these difficult issues is needed. Some research relative to the mechanisms for the trapping phenomena after breather collisions are underway, the base is our study relative to breather collisions in three different Klein-Gordon chains [5, 6].

REFERENCES

- [1] Focus issue edited by S. Flach and R. S. Mackay, *Localization in nonlinear lattices*, Physica D, **119** (1999), 1.
- [2] Focus issue edited by Yu S. Kivshar and S. Flach, *Nonlinear localized modes: physics and applications*, Chaos **13**, (2003), 586.
- [3] Focus issue edited by T. Dauxois, R. S. Mackay and G. P. Tsironis, *Condensed Matter, Dynamical Systems and Biophysics*, Physica D, **216** (2006), 1.
- [4] A. Alvarez, F. R. Romero, J. F. R. Archilla, J. Cuevas and P. V. Larsen, *Breather trapping and breather transmission in a DNA model with an interface*, Eur. Phys. J. B, **51**(2006), 119.
- [5] A. Alvarez, F. R. Romero, J. Cuevas and J. F. R. Archilla, *Discrete moving breather collisions in a Klein-Gordon chain of oscillators*, Phys. Lett. A, **372** (2008), 1256.
- [6] A. Alvarez, F. R. Romero, J. Cuevas and J. F. R. Archilla, *Moving breather collisions in Klein-Gordon chains of oscillators*, Eur. Phys. J. B, **70** (2009), 543.
- [7] S. Aubry, Physica D, *Breathers in nonlinear lattices: existence, linear stability and quantization*, Physica D, **103** (1997), 201.
- [8] S. Aubry and T. Cretegny, *Mobility and reactivity of discrete breathers*, Physica D, **119** (1998), 34.
- [9] D. Campbell, J. Schonfeld and C. Wingate, *Resonance structure in kink-antikink interactions in ϕ^4 theory*, Physica D, **9**(1983), 1.
- [10] D. Chen, S. Aubry and G. P. Tsironis, *Breather mobility in discrete ϕ^4 nonlinear lattices*, Phys. Rev. Lett., **77**(1996), 4776.
- [11] J. Cuevas, J. F. R. Archilla, Yu B. Gaididei and F. R. Romero, *Moving breathers in a DNA model with competing short and long range dispersive interactions*, Physica D, **163** (2002), 106.
- [12] J. Cuevas and J. C. Eilbeck, *Soliton collisions in a waveguide array with saturable nonlinearity*, Phys. Lett. A, **358**(2006), 15.
- [13] J. Cuevas, F. Palmero, J. F. R. Archilla and F. R. Romero, *Moving breathers in a bent DNA-related model*, Phys. Lett. A, **299** (2002), 221.
- [14] J. Cuevas, F. Palmero, J. F. R. Archilla and F. R. Romero, *Moving discrete breathers in a Klein-Gordon chain with an impurity*, J. Phys. A: Math. and Gen., **35** (2002), 10519.
- [15] T. Dauxois and M. Peyrard, *Energy localization in nonlinear lattices*, Phys. Rev. Lett., **70** (1993), 3935.
- [16] T. Dauxois, M. Peyrard and C. R. Willis, *Localized breather-like solutions in a discrete Klein-Gordon model and application to DNA*, Physica D, **57** (1992), 267.
- [17] S. Dmitriev, P. Kevrekidis and Y. Kivshar, *Radiationless energy exchange in three-soliton collisions*, Phys. Rev. E, **78** (2008), 046604.
- [18] Y. Doi, *Energy exchange in collisions of intrinsic localized modes*, Phys. Rev. E, **68** (2003), 066608.
- [19] S. Flach and C. R. Willis, *Discrete breathers*, Phys. Rep., **295** (1998), 181.
- [20] K. Forinash, T. Cretegny and M. Peyrard, *Local modes and localization in a multicomponent nonlinear lattice*, Phys. Rev. E, **55** (1997), 4740.
- [21] K. Forinash, M. Peyrard and B. A. Malomed, *Interaction of discrete breathers with impurity modes*, Phys. Rev. E, **49**(1994), 3400.
- [22] P. G. Kevrekidis, K. Ø. Rasmussen and A. R. Bishop, *The discrete nonlinear Schrödinger equation: a survey of recent results*, Int. J. Mod. Phys. B, **15** (2001), 2833.
- [23] R. S. MacKay and S. Aubry, *Proof of existence of breathers for time-reversible or Hamiltonian networks of weakly coupled oscillators*, Nonlinearity, **7** (1994), 1623.

- [24] J. L. Marín and S. Aubry, *Breathers in nonlinear lattices: numerical calculation from the anticontinuous limit*, *Nonlinearity*, **9** (1996), 1501.
- [25] M. Meister and L. M. Floría, *Bound states of breathers in the Frenkel-Kontorova model*, *Eur. Phys. J. B*, **37** (2004), 213.
- [26] I. E. Papacharalampous, P. G. Kevrekidis, B. A. Malomed and D. J. Frantzeskakis, *Soliton collisions in discrete nonlinear Schrödinger equation*, *Phys. Rev. E*, **68** (2003), 046604.
- [27] M. Peyrard and A. R. Bishop, *Statistical mechanics of a nonlinear model for DNA denaturation*, *Phys. Rev. Lett.*, **62** (1989), 2755.
- [28] B. Sánchez-Rey, G. James, J. Cuevas and J. F. R. Archilla, *Bright and dark breathers in Fermi-Pasta-Ulam lattices*, *Phys. Rev. B*, **70** (2004), 014301.
- [29] M. Sanz-Serna and M. P. Calvo, *Numerical Hamiltonian problems* (Chapman and Hall, 1994).
- [30] A. J. Sievers and S. Takeno, *Intrinsic localized modes in anharmonic crystals*, *Phys. Rev. Lett.*, **61** (1988), 970.

Received xxxx 20xx; revised xxxx 20xx.

E-mail address: azucena@us.es

E-mail address: romero@us.es

E-mail address: jmrr@us.es

E-mail address: archilla.es